Journal of Power Sources 213 (2012) 239–248

Contents lists available at SciVerse ScienceDirect

Journal of Power Sources

journal homepage: www.elsevier.com/locate/jpowsour

Lithium–sulphur batteries – binder free carbon nanotubes electrode examined with various electrolytes

M. Hagen [a,*], S. Dörfler [b], H. Althues [b], J. Tübke [a], M.J. Hoffmann [c], S. Kaskel [b], K. Pinkwart [a]

[a] Fraunhofer Institute for Chemical Technology (ICT), Joseph-von-Fraunhofer-Str. 7, 76327 Pfinztal, Germany
[b] Fraunhofer Institute for Material and Beam Technology (IWS), Winterbergstraße 28, 01277 Dresden, Germany
[c] Karlsruhe Institute for Technology (KIT), Institute for Applied Materials - Ceramics in Mechanical Engineering, Haid-und-Neu-Straße 7, D-76131 Karlsruhe, Germany

ARTICLE INFO

Article history:
Received 26 January 2012
Received in revised form
30 March 2012
Accepted 3 April 2012
Available online 13 April 2012

Keywords:
Lithium–sulphur
Battery
Binder free
Ionic liquid
Solid electrolyte
CNT

ABSTRACT

A new type of electrode for lithium–sulphur batteries is introduced based on vertical-aligned carbon nanotubes (CNTs) grown on a nickel foil without any binder. The electrodes are synthesized by employing a catalyst layer and a CVD process. The CNTs directly synthesized on the Ni current collector are sulphur infiltrated using different approaches and the results are examined by SEM. Furthermore, cycle tests (1.0–3.0 V) with various electrolytes (liquid organic, ionic liquid and solid) are performed.

The binder free CNT cathodes contain the highest so far published total ratio of sulphur (90%) in the electrode. Additionally the sulphur mass per cm^2 electrode can be more than three times as high as in regular slurry-based sulphur electrodes, thus doubling the volumetric energy density.

1. Introduction

Currently used metal-oxide cathodes are regularly toxic, costly and/or low in capacity. By contrast, elemental sulphur is an abundant resource and environmentally friendlier. In comparison to conventional cathode materials, incredibly high capacities of - in theory - 1672 mAh g^{-1} can be achieved in combination with lithium.

During discharge the sulphur cathode is converted into Li_2S. As an intermediate step, lithium polysulphides develop which are soluble in the electrolyte and get further reduced during discharge. While charging, the Li_2S is again converted into highly soluble polysulphides which now get oxidized. Once a voltage between 2.4 and 2.5 V is reached, elemental sulphur is deposited onto the CNT-electrode [1].

One drawback of lithium–sulphur batteries is a shuttle mechanism of lithium-polysulfides between the electrodes, which reduces the efficiency (Fig. 1). Since the polysulphides are dissolved in the electrolyte, long chained ones can diffuse to the lithium electrode and will be reduced in a parasitic reaction. By contrast, short chained polysulphides can diffuse to the "sulphur" electrode and will be oxidized, thus creating a so-called shuttle mechanism [1]. Under certain circumstances this shuttle mechanism could prevent charging to an end of charge voltage where the lithium-polysulfides are completely oxidized to sulphur.

The most effective way to deal with or to influence this shuttle mechanism is the selection of the electrolyte.

Liquid organic electrolytes are the most frequently applied electrolytes for Li–S cells. In order to guarantee the operability of the Li–S cell it is important to use a solvent in which the polysulfides are soluble at least to a certain degree. Popular primary electrolytes are frequently based on tetraethylene glycol dimethyl ether (TEGDME) [2–4] or polyethylene glycol dimethyl ether (PEGDME) [5,6]. Secondary electrolytes consist of two solvents. Usually DME and Dioxolane (DIOX) [7–9] or TEGDME and DIOX [3] are used. N-methyl-N-butyl-piperidinium (PP14) has been examined as an example for an ionic liquid [10]. There are also publications with a combination of ionic liquids and liquid solvent electrolytes [11–14]. Polyethyleneoxide (PEO) is usually used as the polymer backbone in polymer electrolytes for Li–S cells [15–18]. There are also ambitions to construct Li_2S cathodes – a sulphur cathode in discharged state [19,20]. By this means it would be possible to build a cell without

* Corresponding author. Tel.: +49 721 4640 716; fax: +49 721 4640 318.
E-mail address: markus.hagen@ict.fraunhofer.de (M. Hagen).

0378-7753/$ – see front matter © 2012 Elsevier B.V. All rights reserved.
doi:10.1016/j.jpowsour.2012.04.004

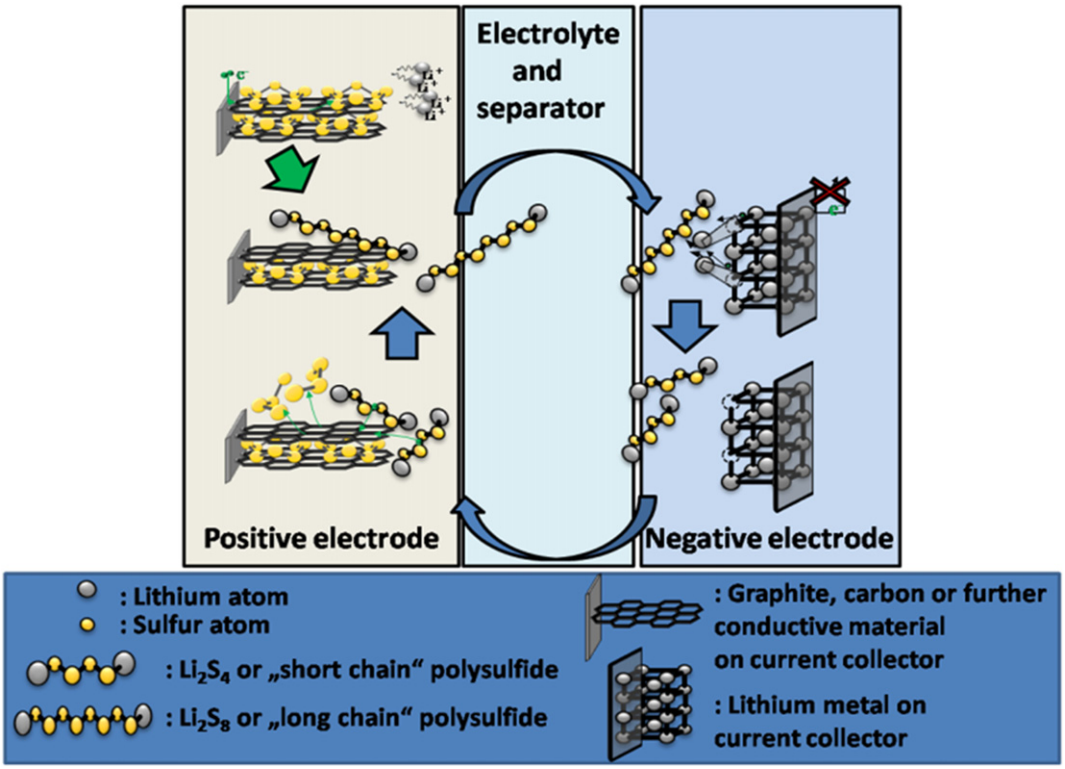

Fig. 1. Polysulfide shuttle mechanism in Li–S cells.

lithium metal and to use alloy anodes or graphite [21]. This could lead to better cell safety and stability, since lithium deposition is not homogenous and can form dendrites which could penetrate or grow around the separator resulting in a shortcut of the cell.

Since sulphur is an insulating material it is necessary to combine it with a conductive matrix. In the past, composites consisting of polyacrylnitrile (PAN) and sulphur have been examined after thermal reaction. The latter deliver more stable capacities in comparison with pure carbon–sulphur electrodes, but the total composition of the electrode usually contain smaller amounts of sulphur (30–50%) [22–27]. As a result, the total electrode capacity is again low, although the capacity referring to the sulphur mass is acceptable (~500–800 mAh g^{-1}). Higher loads of sulphur in the electrode (40–80%) can be obtained through slurry techniques with highly porous carbon, acetylene black, or other carbon conducting agents. CNTs have so far been used as additives in the slurry and have led to more stable capacities during cycling by keeping the integrity of the conductive network [9,28].

In contrast to slurry-based electrodes, vertical-aligned carbon nanotube/sulphur composite electrodes can be directly synthesized on the current collector [29]. Here, we present a VA–CNT-electrode consisting only of CNTs and sulphur without any binder which enables sulphur fractions in the electrode of 0.90 or even higher. The sulphur mass per cm^2 electrode can be more than three times (7.1 mg cm^{-2} for 90% sulphur electrode) as high as in sulphur slurry electrodes with around 2 mg cm^{-2} electrode [30]. The achieved capacities per g sulphur for our CNT electrodes are lower in comparison to electrodes with mesoporous carbon [31] but it seems to be the first approach in which the gravimetric energy density and the volumetric energy density can exceed the lithium-ion level.

2. Experimental

2.1. Preparation of CNT-electrodes

A nickel foil (50 μm and 25 μm thickness, $R_a = 25$ nm, Alfa Aesar, 99% Ni) was used as substrate for the growth of CNTs. The foil was cut into 3.5 × 3.5 cm pieces and dip-coated with aluminium oxide (Al_2O_3) in a process based on a modified sol–gel synthesis [32]. The Al_2O_3 precursor was synthesized by hydrolysis of aluminumisopropoxide ($Al(O–CH(CH_3)_2)_3$) with acetylacetonate as the chelating agent in an aqueous/alcoholic solution to avoid the precipitation of aluminium hydroxide. Two parts of the as synthesized complex solution were diluted by one part 2-propanol. Then 0.05 wt.% cetyltrimethylammonium bromide (CTAB) was added to the complex/2-propanol solution as surfactant to enhance the wettability on the substrate. For the catalyst layer Fe(2-ethylhexanoate)$_3$ (Alfa Aesar, 50% in mineral spirits) and Co(2-ethyhexanoate)$_2$ (Sigma Aldrich, 65% in mineral spirits) were dissolved in 2-propanol (Berkel) to obtain a 0.22 mol l^{-1} solution. Experiments with Mo addition were carried out with Mo(2-ethylhexanoate)$_4$ (Strem Chemicals).

The catalyst and the buffer layer were deposited by a customer-made dip coater. Before coating, the substrates were cleaned with 2-propanol and annealed at 300 °C. The aluminium oxide layer is deposited via 1.0 mm s^{-1} lifting speed; the resulting film is annealed for 5 min at room temperature and 5 min at 300 °C. Subsequently, the catalytic coating is obtained by withdrawing the Al_2O_3-coated substrate from the metal 2-ethylhexanoate solution with a speed of 2.0 mm s^{-1} and by a subsequent thermal treatment at room temperature (5 min) and 350 °C (5 min). A dip-coated layer with 0.22 mol l^{-1} catalyst concentration corresponds to a thickness of approximately 24 nm on 30 nm Al_2O_3.

CNT growth by APCVD was performed with a quartz tube (40 mm diameter) positioned in a split tube furnace (HTM Reetz). The substrate was moved into the quartz tube and annealed with 65 K min^{-1} up to the process temperature of 730 °C. One standard litre per minute (slm) argon (5.0, Linde AG) as carrier gas, 0.17 slm ethene (3.5, Linde AG) as carbon precursor and 0.67 slm hydrogen (5.0, Linde AG) as in situ reductant for the oxidized catalyst layer were used for the carbon nanotube deposition. A small amount of water (85 ppm) as soft oxidant for in situ emerging amorphous carbon plays an important role for the catalyst activity enhancement. Water was transported in the entire gas flow by a stainless steel bubbler with Ar as carrier gas. A growth time of 20 min was applied for all samples being described in this work.

2.2. Sulphur infiltration of CNT-electrodes

In order to infiltrate the CNT electrodes with sulphur the following four methods were evaluated.

2.2.1. Sublimation of sulphur

The test cell described in Fig. 2 was filled with a defined amount of sulphur, and the CNT-electrode was bonded onto the peltier element with a thermally conductive adhesive tape. The peltier element was in electrical contact with two stainless steel stamps. The cell was evacuated and placed in a thermostat at 120 °C until the complete sulphur was below the thermostat solvent level. During the process the upper steel stamp was cooled to properly transport the heat away from the peltier element in order to guarantee a continuous cooling activity of the peltier element. The sublimate sulphur condensed on the cooled CNT-electrode.

2.2.2. Liquefied sulphur

Solid sulphur powder was filled in a glass tube with $d = 0.5$ mm. A heating wire around the glass tube heated the sulphur to a temperature of 150 °C. The liquefied sulphur was dropped onto the CNT-electrode.

2.2.3. Melting of solid sulphur powder

Fine sulphur powder was dispersed on the CNT-electrode and melted on a hot plate in air at 120 °C for 1 min.

2.2.4. Sulphurization through solvent

Sulphur was dissolved in toluol and put on the electrodes by a µ-litre injection. Different temperature constellations have been checked. At room temperature (RT) 40 ml of toluol comprised 0.5 g of sulphur, and hot toluol (80 °C, 40 ml) comprised 2 g sulphur. The CNT-electrode was kept at room temperature or was heated to 120 °C.

The sulphur mass of every single test electrode was weighed with a Mettler Toledo XP205 ($d = 0.01$ mg) by calculating the difference between the bare CNT-Nickel electrode and the sulphurized CNT-Nickel electrode. The sulphur content of every electrode corresponds to the mass fraction.

2.3. Cell assembly and analysis

All tests were conducted against metallic lithium (Sigma Aldrich 99.9% purity) as counter electrode. The lithium was scraped with a ceramic knife in order to remove surface layers and afterwards pressed through a calendar to obtain a homogeneous and reproducible surface. As test cells, glass tubes with screw threads on both sides have been used. For the cell assembling, the lithium foil was cut with a round hollow punch of 10 mm diameter and pressed on a stainless steel stamp with a gasket, which was put in the glass tube. A defined amount of electrolyte was dropped on the polypropylene separator. Afterwards a sulphurized CNT-electrode and a stainless steel disk were placed on the wet separator. A pressure spring put a defined pressure on the electrodes and led to an electrical connection with the second stainless steel stamp. Plastic caps were screwed onto the glass threads to prevent the steel stamps from being pushed out of the cell and to guarantee a proper sealing. The assembly of the test cells took place in

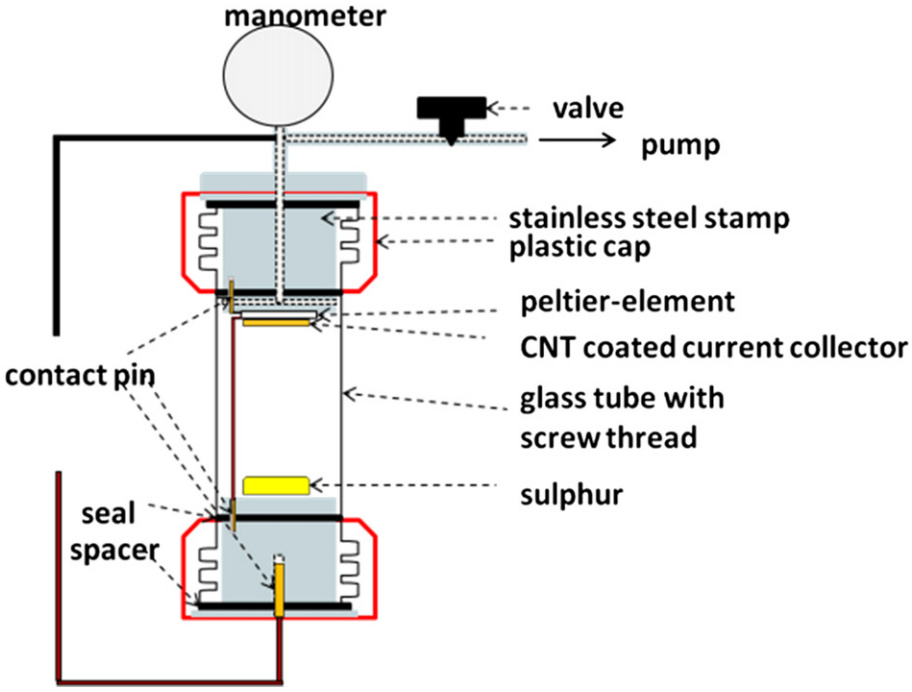

Fig. 2. Cell for vaporizing sulphur which consequently accumulated on the cooled CNT-electrode.

an argon-filled glove box (MBraun) with an O_2 and H_2O content below 1 ppm.

The applied organic and ionic liquid electrolytes consisted of:

- 1M LiTFSI (Sigma Aldrich, 99.95%) in DME:DIOX (1:1, v:v) (Sigma Aldrich, anhydrous)
- 1M LiTFSI in DME:DIOX (1:1, v:v) with 0.25 M $LiNO_3$ (ABCR 99.98%; metals basis)
- 0.7 M kg^{-1} LiTFSI in *N*-buthyl-*N*-methyl-pyrrolidinium TFSI (iolitec) (bmp)

Furthermore, a solid state glass ceramic electrolyte with composition Li_2O–Al_2O_3–SiO_2–P_2O_5–TiO_2–GeO_2 (Ohara, thickness 150 μm, conductivity: 10^{-4} S cm^{-1} at room temperature) was examined with the supporting liquid organic electrolyte 1 M LiTFSI in DME:DIOX (1:1, v:v) for the connection between the electrode and the solid electrolyte. Additionally, the lithium metal anode was separated from the ceramic by a polypropylene separator which was also wetted by the above-mentioned electrolyte. All electrolytes had a water content below 20 ppm.

2.4. Characterization methods

The CNT film or rather the CNT/sulphur composite electrode morphology is characterized by a scanning electron microscope (SEM) (Zeiss type DSM 982 GEMINI) with a heat-able field emission tungsten cathode. The sulphur infiltrated electrodes were characterized by a SEM (Zeiss type EVO MA 10) with Peltier element cooled sample holder and wolfram cathode.

The CNT-S electrodes were cycled between 1.0 V and 3.0 V at constant currents with a Solartron Modu Lab 1450E or a Basytec CTS-LAB. All capacity diagrams show the capacity referring to the weight of sulphur in the electrode, the capacity referring to the weight of the whole composite/electrode (CNT + S) and the capacity referring to the electrode area (m Ah cm^{-2}; right axis) in order to give a good impression of the results quality. The weight of the Ni current collector was not considered for this calculation.

3. Results and discussion

3.1. CNT growth

The Ni substrate with Al_2O_3 layer was dip-coated in different compositions of catalysts (Fe:Mo 47:3 and Fe:Co 2:3) which subsequent formed a particle network layer during thermal annealing. By infusing C_2H_4, H_2 and H_2O in the reaction chamber the single catalyst particles get oversaturated with C defining the CNT diameter by their own diameter.

Fig. 3 shows scanning electron micrographs (SEM) of the as-grown CNT electrodes. In some locations of the CNT film small cracks can be observed caused by the substrate roughness (R_a = 30 nm). The CNT length varies between 100 and 170 μm depending on the catalyst layer composition. The CNTs are multi-walled and have diameters between 8 and 20 nm.

The choice, combination and composition of the catalyst had a great impact on the growth behaviour and density of the CNT layers. Detailed investigations of the CNT growth can be found in [32]. CNT layers grown with the Fe:Co 2:3 system are higher compared to both other systems, but the density is much lower. The catalyst based on Fe:Co 2:3 and Fe leads to multi-walled carbon nanotubes (MWCNT), whereas the catalysts containing 2–8 mol % Mo gives also a low fraction of single walled nanotubes in the MWCNT layer.

3.2. Sulphur infiltration

The target of the different sulphur infiltration approaches was to identify easy and reproducible ways to coat the CNT homogeneously with defined amounts of sulphur.

3.2.1. Sublimation of sulphur

Fig. 4a shows SEM images of a CNT-electrode after sulphur deposition by sublimation according to the sketched cell in Fig. 2. It can be seen that the sulphur coating was not uniform. Sulphur agglomerates as compact particles on the CNT tips, but did not wet the lateral surfaces. The particles had a width and length of around 20 μm–60 μm. Some particles aligned in rows with a length up to 300 μm. In some electrode areas the sulphur accumulated massively. Other electrode regions only showed small amounts of sulphur.

3.2.2. Liquefied sulphur

When the heating wire was set to 150 °C the sulphur formed a yellow drop at the tip of the glass tube that did not leave the tube easily (several tip diameters in the range of 0.1 cm–0.3 cm were examined). After 15 min the CNT-electrode was moved carefully in direction of the sulphur droplet by a height adjustable table until it got in contact. The electrode surface (0.78 cm^2) was immediately covered by a thick sulphur layer and therefore electrically isolated. The sulphur on the electrode weighed 27 mg. As a consequence the approach did not lead to a result that could be examined electrochemically and was not further investigated.

3.2.3. Melting of solid sulphur powder

The sulphur powder was placed onto the CNT which was afterwards put on a heating plate with temperatures between 120 and 150 °C. Within seconds the sulphur became liquid and got

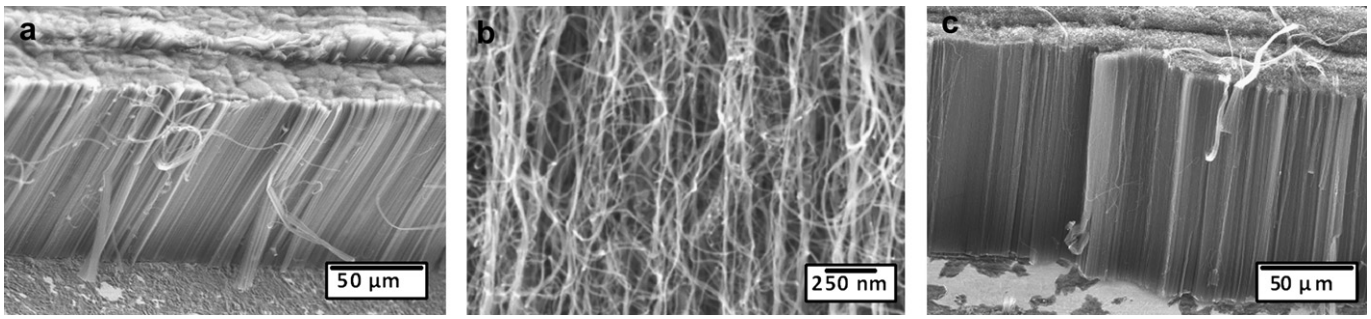

Fig. 3. SEM images in side view of CNTs on Ni current collector with Fe:Mo 47:3 catalyst composition grown at 730 °C for 20 min and magnifcations of a) x500, b) x50.000 and Fe:Co 2:3 catalyst composition grown at 730 °C for 20 min and magnifcations of c) x500.

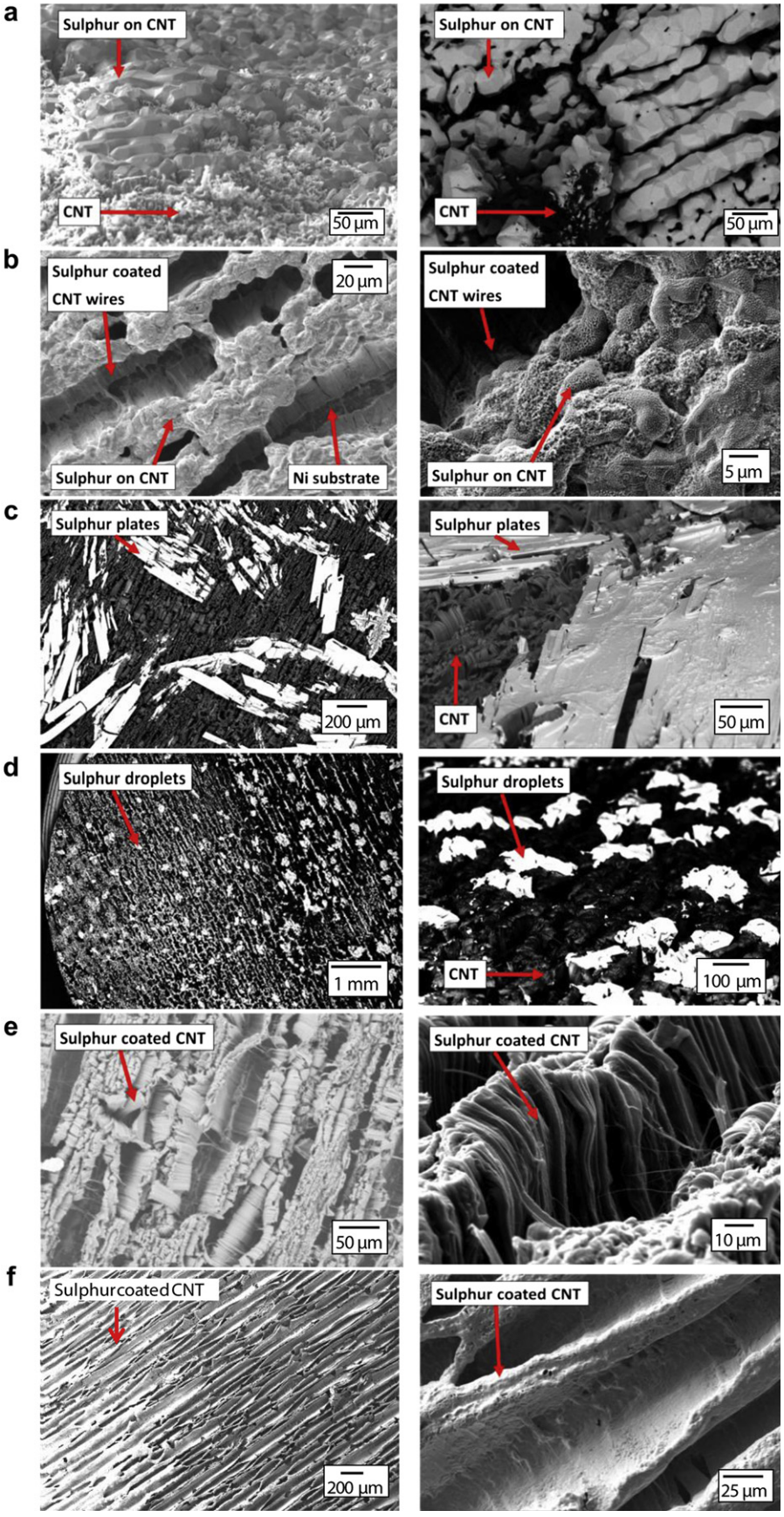

Fig. 4. SEM images of CNT electrodes sulphurized through different techniques at different points of view and different magnifications: a) vaporization of sulphur with subsequent condensation on CNT surface; b) Sulphur powder melted on CNT at 120 °C; c) hot toluol + S solution (80 °C) deposited on RT CNT-electrode; d) RT toluol + S solution deposited on RT CNT-electrode; e) hot toluol + S solution (80 °C) deposited on hot CNT-electrode and f) RT toluol + S solution deposited on hot CNT-electrode.

soaked in the CNT structure. SEM pictures (Fig. 4b) show that the sulphur glued the CNTs together in a channel-like alignment. The sulphur glued CNT channels had a width between 20 and 40 μm and proceeded from one end of the electrode to the other. The sulphur coated both, the lateral surface and the tips of the CNTs. Between the channels "valleys" without CNT and sulphur can be observed. At the bottom of these valleys the Ni substrate is visible.

3.2.4. Sulphurization through solvent

By using hot toluol, greater amounts of sulphur can be carried to the electrode. When the hot toluol/sulphur solution (80 °C) was deposited on a RT CNT-electrode the sulphur immediately formed long, irregularly distributed plates on the top surface of the CNT (Fig. 4c). The plates had a length from 200 to 600 μm and a width between 100 and 300 μm. It was estimated that only one fourth of the electrode area was covered with sulphur. Since the sulphur plates only lay on the CNT tops the contact between the CNT and the sulphur was further seen as weak.

If both, the electrode and the toluol, are at room temperature the results are comparable to the approach with the hot toluol and the RT electrode in the way that the sulphur does not wet the lateral CNT surfaces. The only difference is that the sulphur now forms droplets also located on the tip of the CNT (Fig. 4d). There are bigger droplets with a diameter of around 50 μm and smaller droplets with a diameter of around 10 μm covering in total around 1/3 of the electrode area. As a summary solvent coating with sulphur on room temperature CNT electrodes leads only to non-uniform sulphur coated electrodes with great areas that are not coated at all. Electrochemical experiments with these electrodes delivered poor sulphur utilization and capacity.

If the electrode is heated during sulphur solvent infiltration the sulphur perfectly coats the CNT independently whether hot toluol + sulphur or RT toluol + sulphur are used, as shown in the SEM pictures in Fig. 4e and f. A RT solution is beneficial if the sulphur mass on the electrode requires careful adjustment. A hot toluol solution dissolves larger amounts of sulphur. As a result, the sulphur infiltration process can be accelerated because higher loads of sulphur are dropped on the electrode. Together with a heated electrode, the sulphur coats the complete lateral area of the CNT smoothly. As shown in the SEM pictures the sulphur glues the CNTs together and builds aligned channels crossing the whole electrode. The sulphurized channels have a width of around 20 μm. The valleys between the channels have a width of around 10 μm at the bottom and 40 μm at the top.

As a conclusion, the sulphur infiltration by a solvent in combination with a heated CNT-electrode and the melting of solid sulphur powder delivered much more homogenous and controllable results than the vacuum evaporation approach which is seen to be too complex and expensive for a production. The approach of dropping liquefied sulphur on the electrode led to the electrical isolation of the whole electrode by an uncontrolled mass of sulphur.

Especially the solid powder approach seems to be very interesting for a production process because no solvent is needed that has to be removed from the electrode. Since the CNT electrodes are supposed to be produced by a continuous inline process sulphur infiltration by sulphur powder seems to be promising. In contrary to slurry made electrodes, no long term drying is necessary for the binder free CNT electrodes since the CNT are hydrophobic. The sulphur infiltration by a supporting solvent is seen to be interesting for lab scale because the sulphur mass can be adjusted exactly (+/− 0.1 mg cm^{-2} weight error for one electrode). The electrochemical results of powder and solvent infiltrated electrodes were merely comparable.

4. Electrochemical characterization

The choice of the electrolyte has great influence on cycle stability, achievable capacities, sulphur utilization and the polysulfide shuttle mechanism. Subsequently electrochemical results of Li–S cells with liquid organic electrolytes, ionic liquid electrolytes and solid state electrolytes are described.

4.1. Liquid organic electrolytes

The cycle performance of Li–S cells with 1 M LiTFSI in DME:DIOX (1:1, v:v) and low amounts of sulphur (solvent sulphurization) is compared in Fig. 5. The sulphur content in the electrode was 60% and 69%, and the current density 100 μA cm^{-2} (C/13) and 153 μA cm^{-2} (C/13), respectively. The discharge capacity in the first cycles with 1100 mAh g^{-1} sulphur or 1300 mAh g^{-1} sulphur was high and stayed relatively constant for the next cycles. The charge capacity was always several 100 mAh g^{-1} above the discharge capacity caused by the shuttle effect.

Regarding the surface capacities of the results in Fig. 5 (right axis), the values were clearly below the values of lithium-ion batteries with 2.0–3.0 mAh cm^{-2}. As a consequence, the sulphur mass per electrode had to be enhanced. Since the shuttle

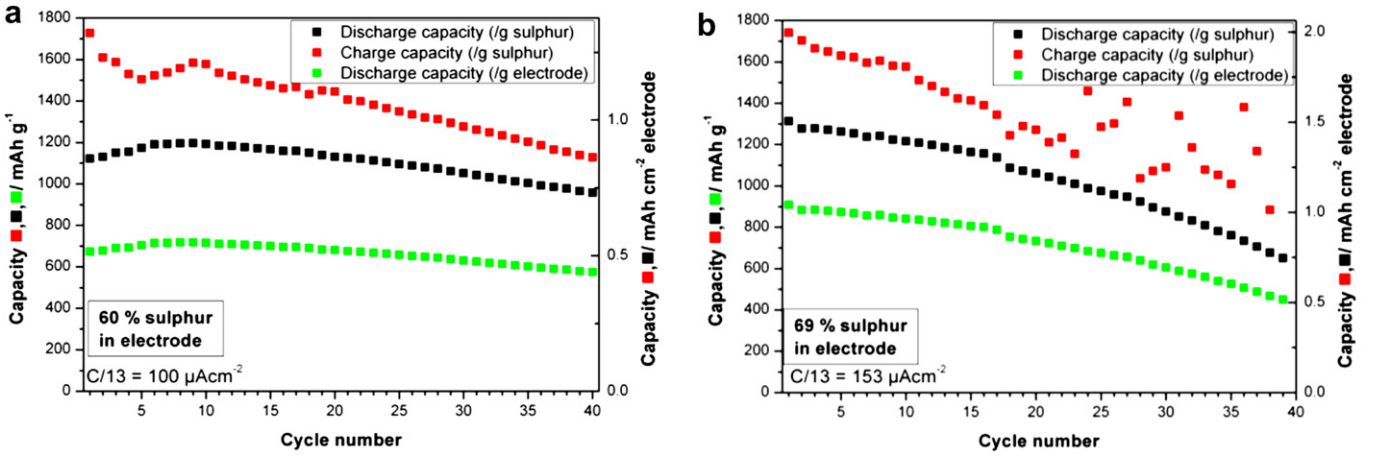

Fig. 5. Capacity over cycle number of a CNT-S electrode with a) 60% sulphur fraction and b) 69% sulphur fraction with liquid organic LiTFSI in DME:DIOX (1:1, v:v). The CNT catalyst was Fe:Co (2:3). The CNT-S electrodes were produced through solvent sulphurization (hot CNT-electrode-RT toluol + sulphur).

mechanism prevented complete charging at higher sulphur loads, 0.25 M $LiNO_3$ was added to the above-mentioned electrolyte. $LiNO_3$ is probably reduced to Li_xNO_y on Li and oxidizes the sulfides to Li_xSO_y species that passivate the Li electrode and thus prevent the continuous transport of electrons from Li to polysulfides in the electrolyte [33]. As a result complete charging until the final end of charge voltage is possible.

By increasing the current density to 0.25 mA cm^{-2} and the sulphur mass to 7.1 mg cm^{-2} electrode (90% sulphur in the electrode), the discharge capacity referred to the sulphur mass decreased to approximately 700 mAh g^{-1}. The calculated surface capacity of approximately 5.5 mAh cm^{-2} is now twice as high as in high-energy lithium-ion batteries or regular sulphur electrodes (Fig. 6a). The U–I-diagram of the electrode with 90% sulphur (Fig. 6b) shows two voltage plateaus during the first discharge at 2.36 V (reduction or decomposition of long chain polysulfides) and 2.10 V (reduction of short chain polysulfides to Li_2S). During the first charge the lower voltage plateau is around 2.22 V (oxidation of Li_2S and short chain polysulfides) and the higher one at 2.38 V (oxidation of long chain polysulfides to sulphur).

Fig. 7 shows a SEM picture of a CNT-S electrode after 20 cycles in the charged state. The electrode was examined after disassembling the test cell in the glove box directly after 24 h of drying in the glove box. The electrode was not cleaned by a solvent and was in contact with air for about 1 min before the SEM was evacuated. The CNT fibres having a length of around 100 μm before electrochemically loading were flattened to a height of around 20 μm through the pressure of the test cell spring and coated by a fine layer that could be identified as sulphur by RAMAN spectroscopy. The CNT network could still be identified through some gaps beneath the sulphur layer (Fig. 7b). Those gaps are probably responsible for the operability of the electrode since they inhibit the complete isolation of the electrode by sulphur or Li_2S even at high loads of sulphur in the cell. The thickness of the sulphur layer is estimated below 50 nm. Another important result of the SEM observation was that the CNT seem to be intact and undamaged and are still in contact with the current collector.

Fig. 8 shows the corresponding RAMAN spectrum of this electrode sealed in an air tight glass cell before drying. The sulphur peaks are clearly visible. Additionally peaks induced by the electrolyte could have been identified by reference spectra of the pure electrolyte (LiTFSI salt and DME, DIOX solvents).

4.2. Ionic liquid electrolyte

The substitution of liquid organic electrolytes by room temperature ionic liquids (ILs) would be an enormous advantage for the cell safety since ionic liquids can be stable up to 300 °C or higher and are not volatile. As a consequence it would be beneficial to identify ILs that are suitable for Li–S cells.

Fig. 10 shows the results of the electrochemical characterization of a CNT-S electrode with 0.7 M kg^{-1} LiTFSI in butyl-methyl-pyrrolidinium (bmp) TFSI at 60 °C. There was only one reduction and oxidation plateau (Fig. 9a) in contrast to the two plateaus for the liquid organic electrolyte (Fig. 6b). This leads to the assumption that the complete reaction mechanism must be different. The current density for charge and discharge was 230 μA cm^{-2} (C/10). The CNT-S electrode contained 64% sulphur. The charge and discharge capacity were around 80 mAh g^{-1} sulphur and stable for 40 cycles. The achieved capacities were unexpectedly low since good results were already published with methyl-buthyl-piperidinium TFSI in [9]. A possible reason could be the choice of the polypropylene separator (Celgard 2400 PP) that may not be suitable for ILs due to the high electrolyte viscosity and low wetting property. However, the electrodes could be charged without any problems to 3 V and the charge and discharge capacity had the same level. This leads to the assumption that no shuttle mechanism took place, probably due to the low solubility of the polysulfides in the IL.

4.3. Solid glass ceramic electrolyte

Glass ceramic electrolytes are stable up to several hundred degree Celsius and are only permeable to lithium ions, making them an ideal candidate to prevent the polysulfide shuttle. Unfortunately, they are currently too expensive, too thick, and not flexible enough. However, the results shown in Fig. 10 demonstrate that solid electrolytes could be an interesting choice for Li–S cells. We utilized a glass ceramic electrolyte with Li_2O–Al_2O_3–SiO_2–P_2O_5–TiO_2–GeO_2 stoichiometry and 150 μm thickness. Since the glass ceramic is not stable against Li, it was separated from Li with a polypropylene Celgard PP 2400 separator which was wetted with 1 M LiTFSI in DME:DIOX (1:1, v:v). For the catholyte room 50 μl of the same liquid organic electrolyte was used in order to contact the CNT-S electrode. The cell was cycled between 1.0 and 3.0 V with a current density of 40 μA cm^{-2} (C/100).

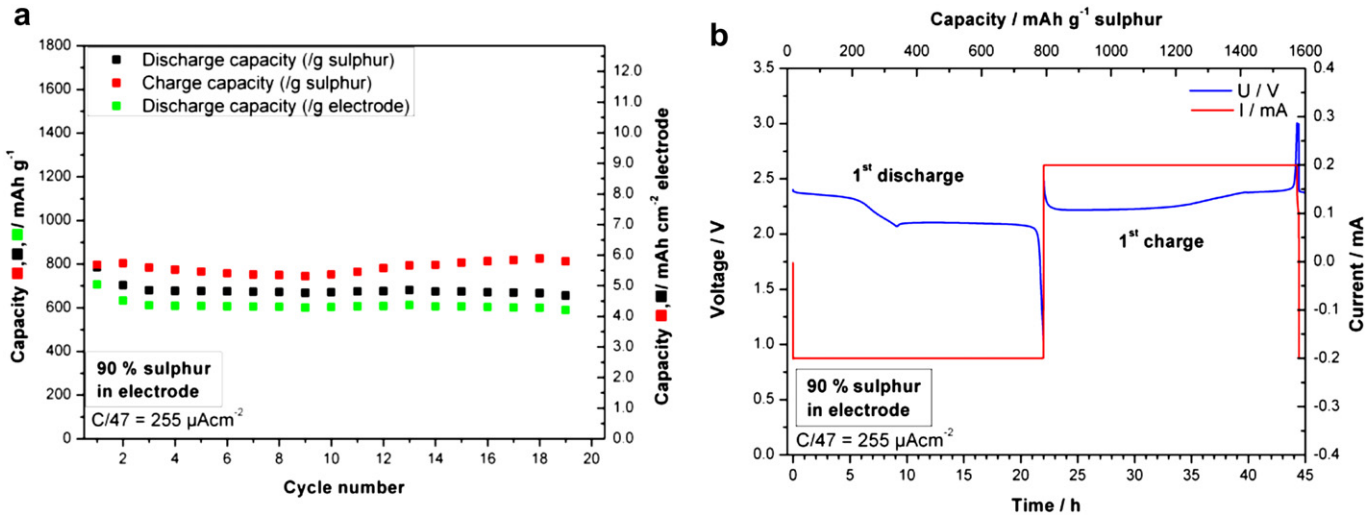

Fig. 6. a) Capacity over cycle number of a 90% sulphur fraction electrode with liquid organic LiTFSI in DME:DIOX (1:1, v:v) + 0.25 M $LiNO_3$ and b) first cycle voltage and current profile of the same electrode. The electrode was produced by melting solid sulphur powder and the CNT catalyst was Fe:Co (2:3).

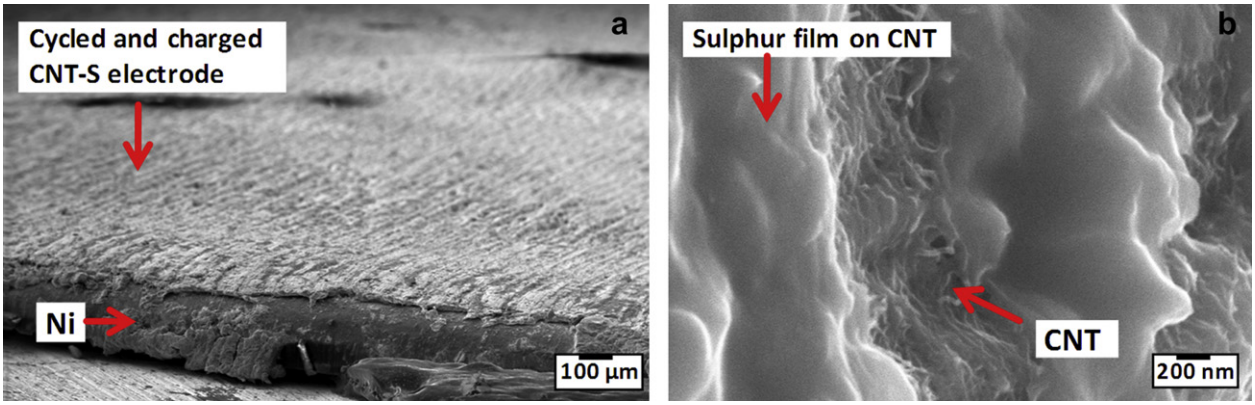

Fig. 7. SEM image of a CNT-S electrode after electrochemical cycling in charged state. The cell was cycled with 1M LiTFSI in DME:DIOX (1:1,v:v) electrolyte.

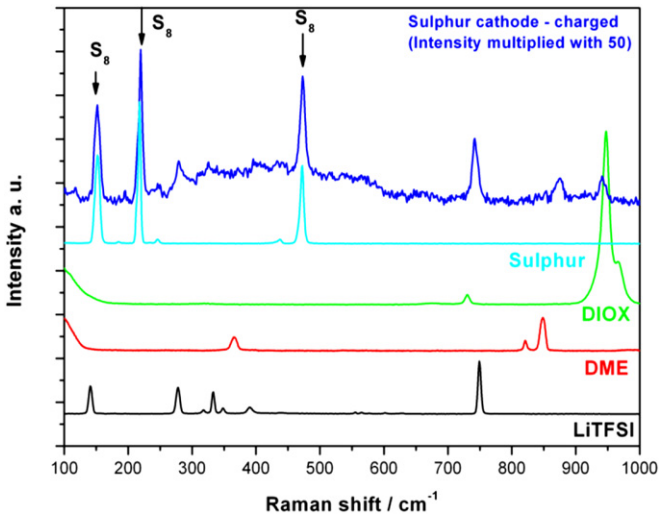

Fig. 8. RAMAN spectrum of the CNT-S electrode shown in Fig. 7 after electrochemical cycling, in charged state with reference spectra. The electrode was cycled with 1 M LiTFSI in DME:DIOX (1:1,v:v) electrolyte.

Although the current density was very low, as expected for a solid electrolyte, there was no or little shuttle mechanism and the cells could be charged to 3 V without any problems even without $LiNO_3$ additive. The charge and discharge capacity were around 1200 mAh g^{-1} sulphur. The first cycle discharge capacity was lower because the cell was not fully charged. The voltage plateau of the discharge was around 2.0 V, but declined during cycling. This could be due to insulating coatings of the solid electrolyte with Li_2S or S increasing the resistance of the cell.

4.4. Sulphur utilization

The achieved capacities with all examined electrodes and electrolytes were always clearly below the possible 1672 mAh g^{-1} sulphur. We believe that this could be due to the following reasons:

Through active material dissolution in the electrolyte the mass of sulphur accumulated on the positive electrode can become lower from cycle to cycle. Regarding the lithium metal anode after disassembling test cells, lithium-sulfide layers can be found on the lithium surface, reducing the original mass of active sulphur step by step. The separator also little contributes to lower capacities, simply by holding a certain amount of electrolyte and polysulfide active mass. Additionally active material can get washed out of the electrode area by adding too much electrolyte. Insufficient electrolyte on the contrary may lead to a too high viscosity and cell impedance,

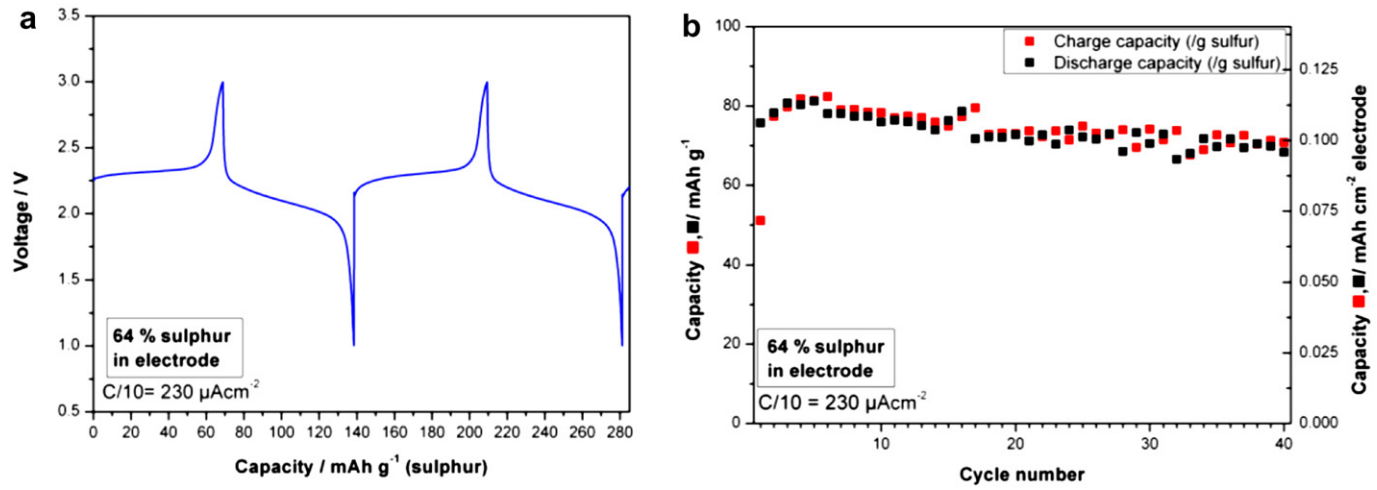

Fig. 9. CNT-S electrode with 64% sulphur fraction and butyl-methyl-pyrrolidinium TFSI electrolyte at 60 °C a) Voltage over capacity and b) capacity over cycle number. The CNT catalyst was Fe:Mo (47:3).

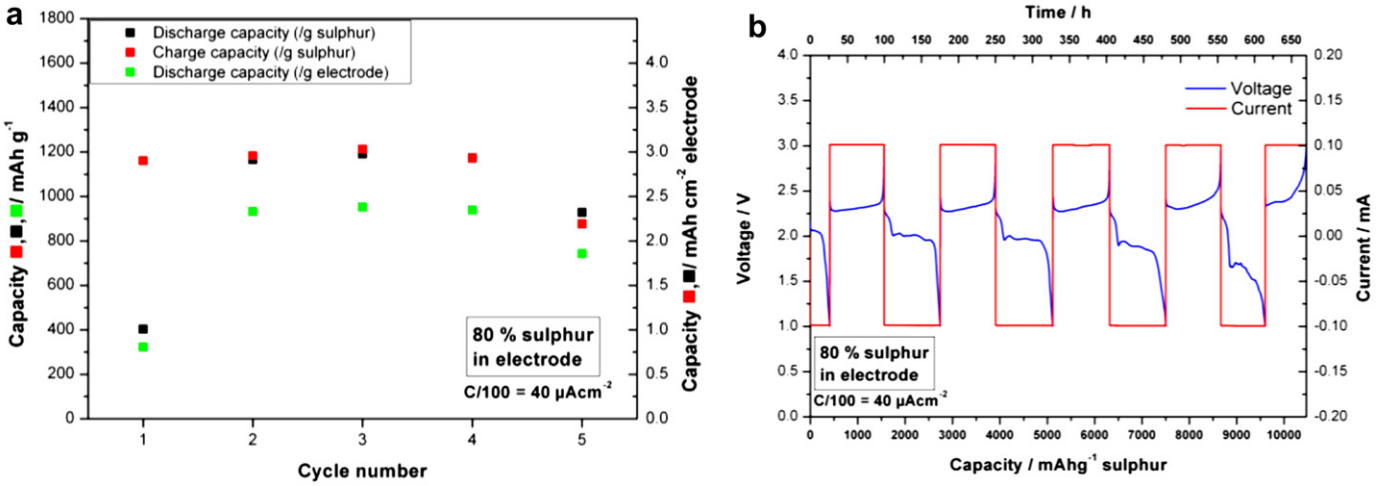

Fig. 10. CNT-S electrode with glass ceramic electrolyte and supporting liquid electrolyte for contact. a) capacity over cycle number b) voltage over capacity. The CNT catalyst was Fe:Co (2:3).

drastically decreasing the achievable capacity. Furthermore the conductive surface of the electrode must be large enough to allow the complete reduction of S_8 to Li_2S.

Since glass tube cells were used in all our experiments it was possible to watch the colour shift of the electrolyte due to polysulfide chain length change. In order to obtain the theoretical capacity of the electrode the electrolyte must have been colourless (contain no lithium-polysulfides) at the end of charge and discharge. That was never the case in our examinations. In order to achieve the theoretical capacity we suggest that the electrode should completely keep hold of the polysulfides. Additionally or as an alternative an electrolyte with low polysulfide solubility can be chosen. Applying a low current to take the slow reaction kinetics into account may now lead to capacities > 1400 mAh g^{-1} sulphur. Nevertheless, the electrode must be able to endure the stress caused by the volume change between sulphur and Li_2S. Otherwise the capacities should fade drastically. We believe that binder free, flexible electrodes can be a good choice for this.

5. Conclusion

A new binder free electrode containing only CNT, directly synthesized on a Ni current collector was introduced as an interesting choice for Li–S cells. The sulphur ratio in the electrode can be raised to 90% and the loads of sulphur per cm^2 electrode can be much higher than in slurry made electrodes. The achieved capacities per g^1 sulphur are below the value of state of the art sulphur electrodes with mesoporous carbon leading to lower gravimetric energy densities. But in contrary the volumetric energy density could be doubled.

Several methods of sulphur infiltration were examined. Good homogenous coatings were achieved by melting solid sulphur powder directly on the CNT-electrode and by solvent sulphurization with a heated CNT-electrode.

The best results concerning the electrode surface capacity were achieved with liquid organic electrolytes and a sulphur ratio of around 90% in the electrode. $LiNO_3$ as an additive in LiTFSI in DME:DIOX enabled the complete charge up to 3 V even at the low applied currents. The achieved surface capacities can be twice as high as in lithium-ion batteries or lithium-sulphur batteries. The examined ionic liquid only had poor capacities of below 100 mAh g^{-1} sulphur. We believe that pure ionic liquid electrolytes may not be suitable for Li–S cells.

An interesting choice for future batteries could be glass ceramics as electrolytes and separators. The examined glass ceramic prevented the shuttle mechanism and allowed charging to 3 V even at a very low current density. Nevertheless, supporting liquid organic electrolyte was used in this test. If the glass ceramics could be produced more cheaply and with a much lower thickness of 20–50 µm they could bring forward the Li–S system.

Acknowledgements

This research was supported by the German Bundesministerium für Bildung und Forschung (BMBF) through the project Fraunhofer Systemforschung für Elektromobilitaet (FSEM).

References

[1] Y.V. Mikhaylik, J.R. Akridge, Journal of the Electrochemical Society 151 (11) (2004) A1969–A1976.
[2] S. Cheon, J. Cho, K. Ko, C. Kwon, D. Chang, H. Kim, S. Kim, Journal of the Electrochemical Society 149 (11) (2002) A1437–A1441.
[3] D. Chang, S. Lee, S. Kim, H. Kim, Journal of Power Sources 112 (2002) 452–460.
[4] H. Ryu, Z. Guo, H. Ahn, G. Cho, H. Liu, Journal of Power Sources 189 (2009) 1179–1183.
[5] J. Wang, J. Chen, K. Konstantinov, L. Zhao, S. Nga, G. Wang, Z. Guo, H. Liu, Electrochimica Acta 51 (2006) 4634–4638.
[6] J. Shim, K.A. Striebel, E. Cairnsa, Journal of the Electrochemical Society 149 (10) (2002) A1321–A1325.
[7] Y. Wang, Y. Huang, W. Wang, C. Huang, Z. Yu, H. Zhang, J. Sun, A. Wang, K. Yuan, Electrochimica Acta 54 (2009) 4062–4066.
[8] L. Qiu, S. Zhang, L. Zhang, M. Suna, W. Wang, Electrochimica Acta 55 (2010) 4632–4636.
[9] L. Yuan, H. Yuan, X. Qiu, L. Chen, W. Zhu, Journal of Power Sources 189 (2009) 1141–1146.
[10] L. Yuan, J. Feng, X. Ai, Y. Cao, S. Chen, H. Yang, Electrochemistry Communications 8 (2006) 610–614.
[11] J. Shin, E. Cairns, Journal of the Electrochemical Society 155 (5) (2008) A368–A373.
[12] M. Rao, X. Song, E.J. Cairns, Journal of Power Sources 205 (2012) 474–478.
[13] S. Kim, Y. Jung, S. Park, Journal of Power Sources 152 (2005) 272–277.
[14] S. Kim, Y. Jung, S. Park, Electrochimica Acta 52 (2007) 2116–2122.
[15] B. Jeon, J. Yeon, K. Kim, I. Chung, Journal of Power Sources 109 (2002) 89–97.
[16] S.S. Jeong, Y.T. Lim, Y.J. Choi, G.B. Cho, K.W. Kim, H.J. Ahn, K.K. Cho, Journal of Power Sources 174 (2007) 745–750.
[17] D. Marmorstein, T.H. Yu, K.A. Striebel, F.R. McLarnon, J. Hou, E.J. Cairns, Journal of Power Sources 89 (2000) 219–226.
[18] X. Zhu, Z. Wen, Z. Gu, Z. Lin, Journal of Power Sources 139 (2005) 269–273.
[19] J. Hassoun, Y. Sun, B. Scrosati, Journal of Power Sources 196 (2011) 343–348.
[20] Y. Yang, M.T. McDowell, A. Jackson, J.J. Cha, Seung Sae Hong, Yi Cui, Nano Letters 10 (4) (2010) 1486–1491.
[21] X. He, J. Ren, L. Wang, W. Pu, C. Wan, C. Jiang, Ionics 15 (2009) 477–481.
[22] X. Yu, J. Xie, J. Yang, K. Wang, Journal of Power Sources 132 (2004) 181–186.

[23] X. Yu, J. Xie, J. Yang, H. Huang, K. Wang, Z. Wen, Journal of Electroanalytical Chemistry 573 (2004) 121–128.
[24] X. Yu, J. Xie, Y. Li, H. Huang, C. Lai, K. Wang, Journal of Power Sources 146 (2005) 335–339.
[25] J.L. Wang, J. Yang, J. Xie, N. Xu, Advanced Materials 14 (2002) 963–965.
[26] J. Wang, J. Yang, C. Wan, K. Du, J. Xie, N. Xu, Advanced Functional Materials 13 (2003) 487–492.
[27] J. Wang, J. Yang, Y. Nuli, R. Holze, Electrochemistry Communications 9 (2007) 31–34.
[28] W. Zheng, Y. Liu, X. Hu, C. Zhang, Electrochimica Acta 51 (2006) 1330–1335.
[29] S. Dörfler, M. Hagen, H. Althues, J. Tübke, S. Kaskel, M.J. Hoffmann, Chemical Communications 48 (2012) 4097–4099.
[30] S.S. Zhang, J.A. Read, Journal of Power Sources 200 (2012) 77–82.
[31] X. Ji, K.T. Lee, L.F. Nazar, Nature Materials 8 (2009) 500–506.
[32] S. Dörfler, A. Meier, S. Thieme, P. Németh, H. Althues, S. Kaskel, Chemical Physics Letters 511 (2011) 288–293.
[33] D. Aurbach, E. Pollak, R. Elazari, G. Salitra, C. Scordilis Kelley, J. Affinito, Journal of the Electrochemical Society 156 (8) (2009) A694–A702.